Research Article

Received: 2 June 2011 Accepted: 30 June 2011 Published online in Wiley Online Library: 7 October 2011

(wileyonlinelibrary.com) DOI 10.1002/pi.3169

Structural symmetry breaking of silicon-containing poly(amide-imide) oligomers and its relation to electrical conductivity and Raman-active vibrations

Carmen M. González Henríquez,[a]* Luis H. Tagle,[a] Claudio A. Terraza,[a] Andrés Barriga González,[b] Ulrich G. Volkmann,[c] Alejandro L. Cabrera,[c] Esteban Ramos-Moore[c] and Maximiliano Pavez-Moreno[c]

Abstract

Optically active poly(amide-imide) oligomers were synthesized by direct polycondensation between an aromatic diamine and a dicarboxylic acid both containing a diphenylsilylene unit. The reaction was carried out using triphenyl phosphite/pyridine in the presence of $CaCl_2$ and *N*-methyl-2-pyrrolidone as solvent. Oligomers were obtained in good yields and showed high solubility in common aprotic polar solvents. The precursors, monomers and poly(amide-imide) oligomers were characterized using elemental analysis and Fourier transform infrared and NMR (^{1}H, ^{13}C, ^{29}Si) spectroscopy. Additionally, the main vibrations of the functional groups (C═O, C═C or N–H) in the oligomers with respect to temperature were characterized using Raman spectroscopy. The glass transition temperature was determined by studying the Raman spectra and corroborated using differential scanning calorimetry. The thermal stability was studied using thermogravimetric analysis. The molecular mass of the compounds was obtained from matrix-assisted laser desorption ionization time-of-flight mass spectrometry and their optical properties were analyzed using UV-visible diode array spectrophotometry. The electronic properties of the oligomers as well as the delocalization of charge carriers within their structures were analyzed using conductance-voltage curves, which showed that these materials are excellent candidates for integrated optoelectronic applications.

Keywords: poly(amide-imide)s; optically active oligomers; Raman spectroscopy; conductance; band gap energy; glass transition

INTRODUCTION

To reach the full potential for application of synthetic poly(amide-imides)s (PAIs) in optoelectronic device fabrication it is necessary to understand the parameters governing their chemical, physical and mechanical properties, such as high-temperature resistance, excellent oxidative stability and good melt processability.[1–4] These compounds are widely used as electronic materials, adhesives, composite materials, and fiber and film materials.[5–12] Additionally, they have been developed as alternative materials offering a compromise between excellent thermal stability, processability, good solubility in highly polar solvents, low glass transition temperatures and easier processability with respect to polyimides.[13,14]

The electronic performance of polymers is intimately connected with the mobility of charge carriers, which in turn depends on the structure and the morphology adopted. Therefore, it is very important to understand and improve the process of molecular ordering and the possibility of obtaining local domains within a system.[15–17] One of the fundamental parameters for characterizing polymers is their glass transition temperature (T_g), involving slow changes in the conformation of the molecules. Raman spectroscopy has additional advantages because it probes simultaneously and '*in situ*' inter- and intramolecular interactions through the self-energy of the vibrations being monitored.[18–22]

Silicon-containing aromatic polymers[23,24] have attracted much scientific and technological interest, because of their potential application in the production of optoelectronic materials. Silicon, when it is placed among aromatic neighbors, introduces a $\sigma-\pi$ conjugation and therefore favors electron transport along macromolecular chains.[25] Thus, the incorporation of silyl groups and optically active structures in a main chain or as side groups can provide a system with an enhancement in solubility, the ability to form higher order structures and counterbalance any loss of thermal stability.[26,27]

In this paper, we report the synthesis of PAI oligomers containing silyl groups in the main chain, from direct polycondensation of four

* *Correspondence to: Carmen M. González Henríquez, Facultad de Química, Pontificia Universidad Católica de Chile, Casilla 306, Santiago 22, Chile. E-mail: cgonzalen@uc.cl*

a *Facultad de Química, Pontificia Universidad Católica de Chile, Casilla 306, Santiago 22, Chile*

b *Facultad de Ciencias Químicas y Farmacéuticas, Universidad de Chile, Av. Vicuña Mackenna 20, Santiago, Chile*

c *Facultad de Física, Pontificia Universidad Católica de Chile, Casilla 306, Santiago 22, Chile*

optically active dicarboxylic acids (**5**), which were synthesized with various derivatives of amino acids (L-alanine (L-Ala), L-leucine (L-Leu), L-valine (L-Val) and L-phenylalanine (L-Phe)), and an aromatic diamine (**6**). These structures were synthesized with the purpose of studying the symmetry breaking of the systems and their physical, thermal and electrical properties. Additionally, elemental analysis values were obtained, and Fourier transform infrared (FTIR) and NMR spectra were analyzed in order to determine the chemical structure of the compounds. The solubility of the PAIs was studied in common organic solvents. The molecular mass was obtained using matrix-assisted laser desorption ionization time-of-flight (MALDI-TOF) mass spectrometry, evidencing oligomeric structures in all cases with two or three repeat units, due to their structural steric hindrance. The glass transition and the thermal stability were studied using DSC and TGA, respectively. This latter technique gives evidence of two types of behavior. On the one hand, more stable molecules, produced by the incorporation of rigid groups, show more resistance to decomposition, even at higher temperatures. On the other hand, the incorporation of flexible chains as pendent groups reduces packing efficiency and leads to a greater degradation of the polymer with respect to higher temperatures. Raman spectroscopy was used to probe the conformation of the stretching modes of the PAI oligomers as a function of temperature. These measurements were corroborated with the T_g values. Furthermore, it is found that these compounds can react with electron acceptors, such as iodine, to form charge transfer species, which increases the electrical conductivity.

EXPERIMENTAL

Materials and equipment

4-Bromo-*o*-xylene, L-Ala, L-Leu, L-Val and L-Phe, 4-bromo-*N*,*N*-bis(trimethylsilyl)aniline, dichlorodiphenylsilane, triphenyl phosphite (TPP) and tosyl chloride (TsCl) were supplied by Sigma-Aldrich (Milwaukee, WI). Anhydrous calcium chloride ($CaCl_2$), lithium and *n*-butyl bromide were obtained from Merck (Darmstadt, Germany). Tetrahydrofuran and diethyl ether were dried by distillation over sodium wire.

The samples were analyzed with the following equipment. FTIR spectra were measured with a PerkinElmer FTIR-1310 spectrometer. 135-DEPT, ^{1}H NMR, ^{13}C NMR and ^{29}Si NMR spectra were recorded with a Bruker 400 MHz spectrometer in deuterated dimethylsulfoxide (DMSO-d_6) or acetone-d_6 as solvent, using tetramethylsilane as an internal standard. The non-modified carbons in 135-DEPT analysis are shown with an asterisk over their chemical shift. Elemental analysis of the precursors, monomers and PAI oligomers was carried out using a Fision EA-1108 instrument. The optical rotation of the compounds was measured at concentrations of 5 and 10 mg dL^{-1} in dimethylformamide (DMF) at 17 °C for monomers and polymers, respectively, using a CIENTEC automatic polarimeter manufactured by Optical Activity Ltd. Melting points were obtained with an SMP3 Stuart Scientific melting point apparatus. Absorption spectra of the PAI oligomers were recorded with an Agilent 8453 diode array spectrophotometer and the band gap energy of the compounds was calculated from their adsorption edges. The absorption spectra were measured at a concentration of 0.5 mg mL^{-1} in DMSO at 25 °C. Molecular masses were estimated using MALDI-TOF mass spectrometry (Microflex, Daltonics Inc., MA). Briefly, from polymer solutions at about 1.5 mg mL^{-1} in acetone were prepared various dilutions with 2,5-dihydrobenzoic acid as matrix prepared at a concentration of 10 mg mL^{-1} in acetone and then deposited on a steel plate (dried droplet method). Spectra were acquired at various *m/z* intervals as sums of 500 accumulated laser shots.

DSC traces were recorded with a Mettler Toledo DSC 821e differential scanning calorimeter and thermal degradation temperatures with a TGA/SDTA 851e Mettler Toledo thermobalance. Both analyses were recorded at a heating rate of 20 °C min^{-1} under nitrogen atmosphere.

Raman spectroscopy was performed with a LabRam 010 instrument from ISA using a 5.5 mW HeNe laser beam (633 nm) without a filter. The Raman microscope used a backscattering geometry, where the incident beam was linearly polarized and the spectral detection unpolarized. The objective lens of the microscope was an Olympus Mplan ×100, and the integration time for each spectrum was 8 s, except for the measurement of sample PALV (60 s). A Linkam TMS 94 controller and THMS 600 stage were used to vary the sample temperature with a precision of ±0.1 °C. The temperature was varied with a heating rate of 20 °C min^{-1}, and before taking a spectrum the temperature was stabilized for 30 s to ensure that the sample was in equilibrium with the stage. For sample preparation, polymer powder (20 mg) was cast on glass slides. It was then heated to 200 °C for 1 min. The temperature was subsequently decreased to −170 °C and again increased above the corresponding T_g.

An RT66B electronic tester from Radiant Technologies Inc. was used to measure current–voltage curves in order to study the conductance of the PAI oligomers. Silver electrodes were deposited by physical vapor deposition (PVD) on pellets of PAI oligomers, fabricated with a pressure of 10 tons.

Synthesis of precursors and monomers (Scheme 1)

Bis(3,4-dicarboxyphenyl)diphenylsilane dianhydride (**4**) was prepared by a multistep reaction.[27–29] 4-Bromo-*o*-xylene (**1**) was reacted with diphenyldichlorosilane to produce bis(3,4-dimethylphenyl)diphenylsilane (**2**). The aqueous potassium permanganate/pyridine oxidation of the latter gave, after neutralization, the corresponding bis(3,4-dicarboxyphenyl)diphenylsilane (**3**), which was then dehydrated in refluxing acetic anhydride to afford the corresponding dianhydride (compound **4**). The new dicarboxylic acids (**5a**–**5d**) were prepared according to a methodology previously described.[30]

(2*R*, 2′*S*)-2,2′-(5,5′-(Diphenylsilanediyl)bis(1,3-dioxoisoindoline-5,2-diyl))dipropanoic acid (**5a**). Yield: 51%, m.p.: 152.3–155.1 °C. FTIR (KBr; cm^{-1}): 3467 (O–H stretching), 3070 (C–H arom. stretching), 2945 (CH_3, C–H stretching), 1716 (C═O amide stretching), 1450 (Si–C arom. stretching), 1428 (C–O–H bending), 1414 (CH_3 bending), 1316, 1220 (O–C stretching), 701 (C–H arom. 'out of plane' (*oop*) bending). ^{1}H NMR (DMSO-d_6; δ, ppm): 7.98 (s, 4H, Ph–*H*), 7.83 (s, 2H, Ph–*H*), 7.55–7.47 (m, 10H, Ph–*H*), 4.85–4.84 (m, 2H, CH), 1.51–1.49 (dd, 6H, CH_3). ^{13}C NMR (DMSO-d_6; δ, ppm): 171.4, 167.6, 167.4 (C═O), 142.7*, 141.5, 136.4*, 134.6, 133.9, 133.3, 131.3*, 129.9*, 129.2*, 123.5* (10 C arom.), 47.5* (CH), 15.2* (CH_3). ^{29}Si NMR (DMSO-d_6; δ, ppm): −13.8 ppm. Elemental analysis: ($C_{34}H_{26}N_2O_8Si$) (618.66): calcd C 66.01, H 4.24, N 4.53, O 20.69; found C 63.86, H 5.63, N 4.43. $[\alpha]_{589}^{17} = -20.0^{\circ}$ dm^{-1} g^{-1} cm^3.

(2*R*, 2′*S*)-2,2′-(5,5′-(Diphenylsilanediyl)bis(1,3-dioxoisoindoline-5,2-diyl))bis(4-methylpentanoic acid) (**5b**). Yield: 56%, m.p.: 142.9–145.0 °C. FTIR (KBr; cm^{-1}): 3429 (O–H stretching), 3070–3051 (C–H arom. stretching), 2959, 2933 (C–H aliph. stretching), 1719 (C═O amide stretching), 1469 (Si–C arom.), 1428 (C–O–H bending), 1414 (C–H aliph. bending), 1316, 1262 (O–C, stretching), 700 (C–H arom. *oop* bending). ^{1}H NMR

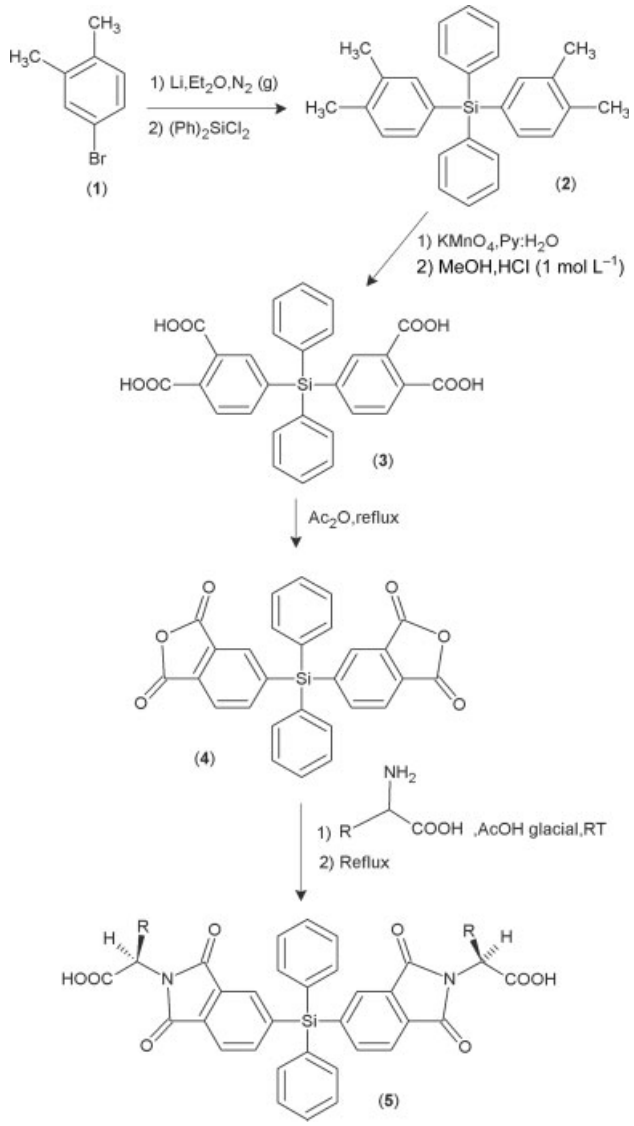

Scheme 1. Synthesis of dicarboxylic acid chiral monomers where R = H_3C–(**5a**), $(CH_3)_2CHCH_2$–(**5b**), $(CH_3)_2CH$–(**5c**) and $PhCH_2$–(**5d**). Py : H_2O (2 : 3 vol/vol), C($KMnO_4$) = 1.0 mol/L.

(DMSO-d_6; δ, ppm): 7.99 (t, 4H, Ph–*H*), 7.84 (s, 2H, Ph–*H*), 7.55–7.47 (m, 10H, Ph–*H*), 4.77–4.73 (dd, 2H, CH–N), 2.15–2.09 and 1.82–1.76 (t, 4H, CH_2), 1.43–1.41 (s, 2H, $CH(CH_3)_2$), 0.82 (t, 12H, CH_3). ^{13}C NMR (DMSO-d_6; δ, ppm): 171.2, 167.9 (C═O), 142.9*, 139.6*, 133.1, 132.6, 131.9, 131.3*, 130.1*, 129.2*, 126.5, 123.6* (10C arom.), 50.7* (CH–N), 37.9* (CH_2), 24.9*($CH(CH_3)_2$), 23.7* (CH_3). ^{29}Si NMR (DMSO-d_6; δ, ppm): −13.90. Elemental analysis: ($C_{40}H_2N_2O_8Si$) (702.82): calcd C 68.36, H 5.45, N 3.99, O 18.21; found C 66.63, H 7.53, N 4.00. $[\alpha]_{589}^{17} = -19.6^\circ$ dm^{-1} g^{-1} cm^3.

(2*R*, 2′*S*)-2,2′-(5,5′-(Diphenylsilanediyl)bis(1,3-dioxoisoindoline-5,2-diyl))bis(3-methylbutanoic acid) (**5c**). Yield: 51%, m.p.: 143.7–146.7 °C. FTIR (KBr; cm^{-1}): 3475 (O–H stretching), 3070–3050 (C–H arom. stretching), 2966 (CH_3, C–H stretching), 1729 (C═O amide stretching), 1469 (Si–C arom.), 1428 (C–O–H bending), 1414 (CH_3 bending), 1210 (O–C stretching), 700 (C–H arom. *oop* bending). ^{1}H NMR (DMSO-d_6; δ, ppm): 8.00 (t, 4H, Ph–*H*), 7.85 (s, 2H, Ph–*H*), 7.54–7.47 (m, 10H, Ph–*H*), 4.45–4.43 (dd, 2H, CH–N), 2.53–2.51 (m, 2H, $CH(CH_3)_2$), 1.03–1.01 and 0.80–0.79 (dd, 12H, CH_3). ^{13}C NMR (DMSO-d_6; δ, ppm): 170.13, 167.98, 167.81 (C═O), 142.9*, 141.7, 138.8, 136.5*, 133.0, 131.3*, 130.9, 130.1*, 129.2*, 123.6* (10C arom.), 57.5* (CH–N), 28.4*, 21.3* ($CH(CH_3)_2$), 19.7* (CH_3). ^{29}Si NMR (DMSO-d_6; δ, ppm): −13.89. Elemental analysis: ($C_{38}H_{34}N_2O_8Si$) (674.77): calcd C 67.64, H 5.08, N 4.15, O 18.97; found C 65.74, H 6.82, N 4.10. $[\alpha]_{589}^{17} = -53.7^\circ$ dm^{-1} g^{-1} cm^3.

(2*R*, 2′*S*)-2,2′-(5,5′-(Diphenylsilanediyl)bis(1,3-dioxoisoindoline-5,2-diyl))bis(3-phenylpropanoic acid) (**5d**). Yield: 62%, m.p.: 134.4–138.0 °C. FTIR (KBr; cm^{-1}): 3408 (O–H stretching), 3066–3027 (C–H arom. stretching), 2928 (CH_2, C–H stretching), 1717 (C═O amide stretching), 1497 (Si–C arom.), 1428 (C–O–H bending), 1414 (CH_2 bending), 1319, 1261 (O–C stretching), 699 (C–H arom. *oop* bending). ^{1}H NMR (DMSO-d_6; δ, ppm): 7.93–7.90 (t, 4H, Ph–*H*), 7.74 (s, 2H, Ph–*H*), 7.46–7.52 (m, 10H, Ph–*H*), 7.13–7.08 (m, 10H, Ph–*H*), 5.13–5.09 (dd, 2H, CH), 3.48–3.44 and 3.34–3.31 (dd, 4H, CH_2). ^{13}C NMR (DMSO-d_6; δ, ppm): 170.45, 167.60, 167.43 (C═O), 143.0*, 141.8, 137.8, 136.43*, 132.7, 131.3*, 131.1, 130.6, 130.0*, 129.2*, 128.8*, 127.1*, 124.5*, 123.6* (14C arom.), 53.6* (CH), 34.4* (CH_2). ^{29}Si NMR (DMSO-d_6; δ, ppm): −14.0. Elemental analysis: ($C_{46}H_{34}N_2O_8Si$) (770.86): calcd C 71.67, H 4.45, N 3.63, O 16.60; found C 69.83, H 6.22, N 3.80. $[\alpha]_{589}^{17} = -76.9^\circ$ dm^{-1} g^{-1} cm^3.

Bis(4-aminophenyl)diphenylsilane (**6**) was prepared according to a procedure described in the literature.[28,31]

Synthesis of PAI oligomers

A typical polycondensation is shown in Scheme 2, and was carried out as follows.[32,33] A mixture of **5a** (0.38 g, 0.62 mmol), diamine **6** (0.23 g, 0.62 mmol), 0.15 g of $CaCl_2$, 0.45 mL of TPP, 0.40 mL of pyridine and 0.75 mL of *N*-methyl-2-pyrrolidone (NMP) was heated while being stirred at 110 °C for 3 h. The flask was cooled to room temperature, and the mixture was poured into methanol. The PAI oligomer (PALA) was reprecipitated from a DMSO solution using methanol. The solid obtained was filtered off, washed with methanol, dried under vacuum for 12 h and characterized.

PALA. Yield: 90%. FTIR (KBr; cm^{-1}): 3361 (N–H stretching), 3068–3023 (C–H arom. stretching), 2939 (CH_3, CH stretching), 1774 (C═O imide stretching), 1717 (C═O amide stretching), 1592 (C═C arom. bending), 1514 (Si–C arom.), 1428–1412 (CH_3 scissoring, bending), 1188, 1110, 1067 (C–H arom. 'in plane' (*ip*) bending, ring torsion), 700 (C–H arom. *oop* bending). Raman at room temperature (cm^{-1}): 1773 (C═O stretch), 1608, 1513, 1409 (ring stretching), 1593 (Si–C arom.), 1588 (N–H bending, secondary amide), 1187, 1027 (C═C arom. *ip* bending), 936–990 (C═C arom. *oop* deformation). ^{1}H NMR (DMSO-d_6; δ, ppm): 7.98 (s, 2H, Ph–*H*), 7.89 (s, 2H, NH), 7.59–6.70 (m, 32H, Ph–*H*), 4.89 (m, 2H, CH–N), 1.54 (d, 3H, CH_3). ^{13}C NMR (DMSO-d_6; δ, ppm): 169.95, 168.35, 167.68 (C═O), 139.5, 137.5, 136.4*, 136.2*, 135.5*, 135.4, 135.0, 133.9, 133.3, 131.9, 131.3*, 130.0*, 129.2*, 129.0*, 128.7*, 128.6*, 120.1*, 120.0* (18C arom.), 49.3* (CH), 21.8* (CH_3). ^{29}Si NMR (DMSO-d_6; δ, ppm): −13.9. Elemental analysis: ($C_{57}H_{41}N_4O_6Si_2$) $(933.79)_n$: calcd C 73.31, H 4.39, N 6.00; found C 72.83, H 4.02, N 5.38. $[\alpha]_{589}^{17} = -9.0^\circ$ dm^{-1} g^{-1} cm^3.

PALL, PALV and PALPHA were obtained from **5b, 5c** and **5d**, respectively, following a similar procedure.

PALL. Yield: 83%. FTIR (KBr; cm^{-1}): 3433 (N–H stretching), 3069 (C–H arom. stretching), 2958–2871 (CH_3, CH_2, CH stretching), 1773 (C═O imide stretching), 1718 (C═O amide stretching), 1592 (C═C arom. bending), 1511 (Si–C arom.), 1428–1412 (CH_3 scissoring, bending), 1188, 1110, 1079 (C–H arom. *ip* bending, ring torsion), 741 (CH_2 rocking bending), 700 (C–H arom. *oop* bending). Raman at room temperature (cm^{-1}): 3047 (C–H arom. stretching), 2962

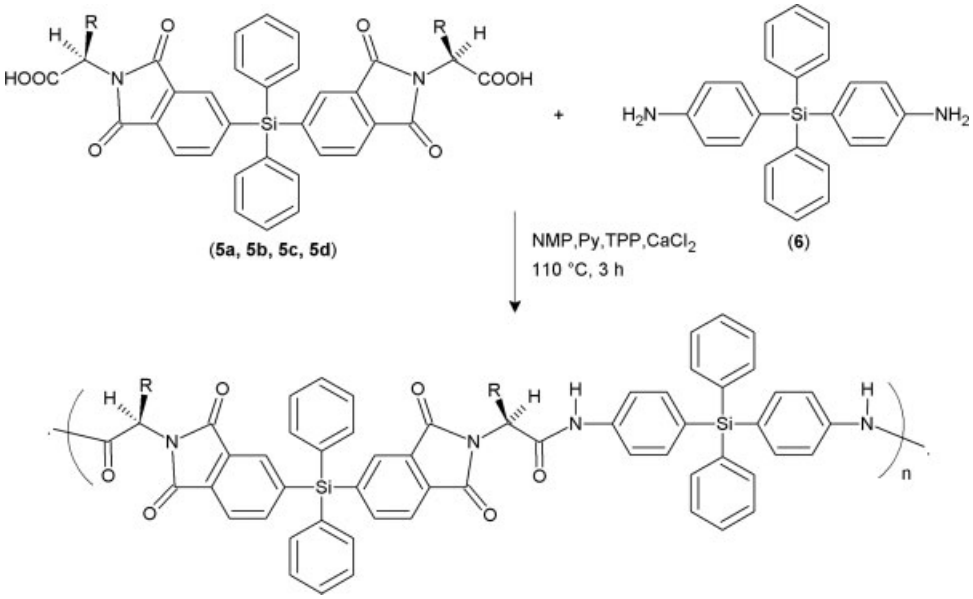

Scheme 2. Synthesis of PAI oligomers obtained by condensation, where R = H_3C- (PALA), $(CH_3)_2CHCH_2-$ (PALL), $(CH_3)_2CH-$ (PALV) and $PhCH_2-$ (PALPHA).

(CH_3, CH_2, CH stretching), 1772 (C=O stretching), 1611, 1513, 1411 (ring stretching), 1589 (Si–C arom.), 1585 (N–H bending, secondary amide), 1189, 1028 (C=C arom. *ip* bending), 936–990 (C=C arom. *oop* deformation). ^{1}H NMR (DMSO-d_6; δ, ppm): 8.00 (s, 2H, Ph–*H*), 7.83 (s, 2H, NH), 7.60–6.71 (m, 32H, Ph–*H*), 4.89–4.87 (d, 2H, CH–N), 2.16–2.14 and 1.92 (t, 4H, CH_2), 1.41 (m, 2H, C*H*$(CH_3)_2$), 0.85–0.83 (dd, 12H, CH_3). ^{13}C NMR (DMSO-d_6; δ, ppm): 171.9, 168.3, 168.3 (C=O), 139.0, 138.0, 136.8*, 136.4*, 136.2, 133.7, 133.6, 133.4, 131.3, 131.2*, 131.0, 130.0*, 129.2*, 129.0*, 128.7*, 128.6*, 128.4*, 120.1* (18C arom.), 52.7* (CH–N), 37.4* (CH_2), 25.2* (C*H*$(CH_3)_2$), 23.7* (CH_3). ^{29}Si NMR (DMSO-d_6; δ, ppm): −13.9. Elemental analysis: $(C_{60}H_{47}N_4O_6Si_2)$ $(975.82)_n$: calcd C 73.85, H 4.82, N 5.74; found C 72.77, H 4.11, N 5.06. $[\alpha]_{589}^{17} = -9.6^\circ$ dm^{-1} g^{-1} cm^3.

PALV. Yield: 85%. FTIR (KBr; cm^{-1}): 3433 (N–H stretching), 3069 (C–H arom. stretching), 2965 (CH_3, C–H stretching), 1774 (C=O imide stretching), 1712 (C=O amide stretching), 1592 (C=C arom. bending), 1518 (Si–C arom.), 1428 (CH_3 scissoring, bending), 1188, 1110, 1076 (C–H arom. *ip* bending, ring torsion), 700 (C–H arom. *oop* bending). Raman at room temperature (cm^{-1}): 3056 (C–H arom. stretching), 1773 (C=O stretching), 1607, 1513, 1413 (ring stretching), 1593 (Si–C arom.), 1586 (N–H bending, secondary amide), 1193, 1026 (C=C arom. *ip* bending), 925 (C=C arom. *oop* deformation). ^{1}H NMR (DMSO-d_6; δ, ppm): 7.98 (s, 2H, Ph–*H*), 7.82 (s, 2H, NH), 7.60–6.71 (m, 32H, Ph–*H*), 4.52 (d, 2H, CH–N), 2.78 (m, 2H, C*H*$(CH_3)_2$), 0.98 and 0.81 (dd, 12H, CH_3). ^{13}C NMR (DMSO-d_6; δ, ppm): 171.8, 168.3, 168.0 (C=O), 142.7, 141.4, 136.4*, 136.2*, 135.4*, 134.6, 134.4, 133.6, 131.3, 131.0*, 130.0*, 129.2*, 129.0*, 128.8, 128.7*, 128.5*, 120.1*, 119.9* (18C arom.), 36.1* (CH–N), 20.9* (C*H*$(CH_3)_2$), 19.7* (CH_3). ^{29}Si NMR (DMSO-d_6; δ, ppm): −13.9. Elemental analysis: $(C_{59}H_{45}N_4O_6Si_2)$ $(961.81)_n$: calcd C 73.67, H 4.68, N 5.83; found C 73.03, H 4.09, N 5.14. $[\alpha]_{589}^{17} = -17.2^\circ$ dm^{-1} g^{-1} cm^3.

PALPHA. Yield: 78%. FTIR (KBr; cm^{-1}): 3386 (N–H amide stretching), 3067–3026 (C–H arom. stretching), 2924 (CH_3, CH_2, C–H stretching), 1774 (C=O imide stretching), 1718 (C=O amide stretching), 1592 (C=C arom. bending), 1514 (Si–C arom.), 1428 (CH_3, CH_2 scissoring, bending), 1188, 1111, 1063 (C–H arom. *ip* bending, ring torsion), 741 (CH_2 rocking bending), 699 (C–H arom. *oop* bending). Raman at room temperature (cm^{-1}): 3050 (C–H arom. stretching), 2919 (CH_3, CH_2, C–H stretching), 1771 (C=O stretching), 1608, 1509, 1412 (ring stretching), 1594 (Si–C arom.), 1588 (N–H bending, secondary amide), 1322, 1240 ($-CH_2-$wag), 1154, 1058 (C=C arom. *ip* bending), 996 (C=C arom. *oop* deformation), 832 ($-CH_2-$rock). ^{1}H NMR (DMSO-d_6; δ, ppm): 7.91 (s, 2H, Ph–*H*), 7.68 (s, 2H, NH), 7.62–6.71 (m, 42H, Ph–*H*), 5.15 (t, 2H, CH–N), 3.57–3.54 (d, 4H, CH_2). ^{13}C NMR (DMSO-d_6; δ, ppm): 169.28, 155.18, 153.76 (C=O), 138.88, 137.89, 136.85*, 136.37*, 136.21*, 135.40*, 134.42, 132.89, 132.00, 131.26*, 131.17, 131.00*, 130.25, 130.04*, 129.71, 129.35*, 129.19*, 128.74*, 127.03*, 123.44*, 120.81*, 120.17* (22C arom.), 55.39* (CH), 34.57* ppm (CH_2). ^{29}Si NMR (DMSO-d_6; δ, ppm): −14.0. Elemental analysis: $(C_{63}H_{45}N_4O_6Si_2)$ $(1009.85)_n$: calcd C 74.92, H 4.46, N 5.55; found C 73.65, H 4.31, N 4.98. $[\alpha]_{589}^{17} = -58.2^\circ$ dm^{-1} g^{-1} cm^3.

RESULTS AND DISCUSSION

The structure of the repeat unit of each PAI oligomer was satisfactorily established by elemental analysis and spectroscopic techniques: FTIR, Raman and NMR. These results are summarized in the preceding section.

Solubility of the PAI oligomers

The solubility of the PAI oligomers at room temperature was investigated in various solvents. All the samples exhibit a good solubility in a variety of aprotic polar solvents such as acetone, DMF, *N*,*N*-dimethylacetamide, NMP and DMSO, but they are also soluble in less polar solvents like pyridine, *m*-cresol, tetrahydrofuran and CH_2Cl_2. In contrast, the PAI oligomers are insoluble in some polar protic and non-polar solvents such as water, methanol, ethanol, CCl_4, hexane and diethyl ether. Moreover, these samples are soluble in 1,4-dioxane, $CHCl_3$ and benzene and partially soluble in toluene.

Optical properties: effect of doping

The UV-visible spectra of the PAI oligomers without doping reveal a strong absorption band at 261 nm and a weaker one at 308 nm

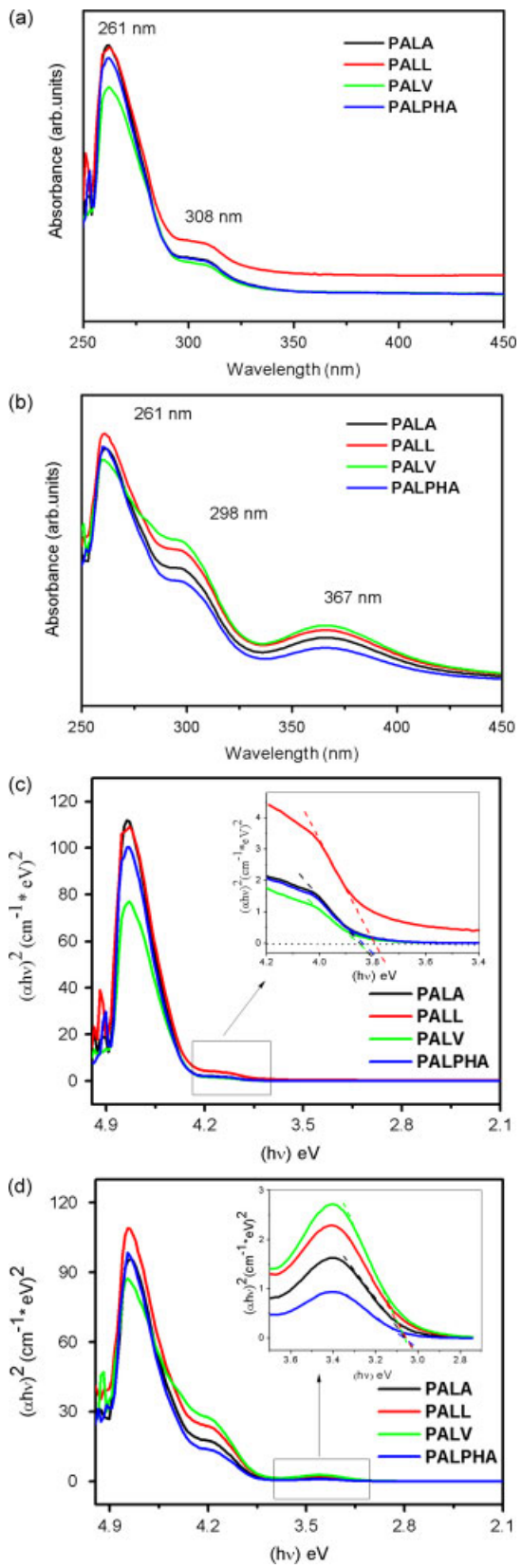

Figure 1. UV-visible absorption spectra (PAI oligomers dissolved at 25 °C in DMSO): (a) without doping; (b) with doping. Band gap energy of samples: (c) without doping; (d) with doping.

Table 1. Variation of direct band gap energies for the PAI oligomers

Oligomer	Band gap (eV)[a] without doping, direct (308 nm)	Band gap (eV)[a] with doping, direct (367 nm)
PALA	3.85	3.06
PALL	3.79	3.05
PALV	3.85	3.06
PALPHA	3.84	3.06

[a] Taken from the UV-visible absorption spectra.

(Fig. 1(a)). These bands correspond to $\pi-\pi$ charge transfer, with a strong aromatic acceptor. When the samples are exposed to iodine vapor for some days, the color of the solids changes from light to dark brown with increasing dopant content. These changes are produced by the diffusion of dopant molecules into the oligomeric structure, implying the formation of a charge transfer complex. After doping, an absorption peak appears at about 367 nm, indicating the formation of a new conjugated structure, related to the delocalized electrons, which can be found in conjugated systems of polymers (Fig. 1(b)).

The optical band gap energy (E_g) between the valence band and the conduction band was obtained from the UV-visible absorption spectra, using the Tauc expression[34,35]

$$\alpha = \frac{b(h\nu - E_g)^{1/2}}{h\nu} \quad (1)$$

This equation involves the optical absorption coefficient α, which determines the optical energy gap, as a function of photon energy $h\nu$ and b is a constant. The term 1/2 in this equation is related to materials with a direct allowed transition.[36]

The optical absorption coefficient was calculated using

$$\alpha = \frac{2.303A}{l} \quad (2)$$

which corrects the reflection losses. Parameter A is the absorbance and l is the optical path length ($l = 1$ cm).[37] Then, by plotting $(\alpha h\nu)^2$ *versus* $h\nu$ it is possible to obtain the direct gap from extrapolation of the linear portion of the plot to the energy axis (Figs 1(c) and (d)).

The influence of the chemical structure on the conformation of the chains is related to the band gap.[38] The intrinsic band gap of undoped PAI oligomers shows a higher value (3.85–3.79 eV at 308 nm; Fig. 1(c)) than that of doped samples (3.06–3.05 eV at 367 nm; Fig. 1(d)). This property might be related to the torsion between the adjacent rings in the monomeric units (Scheme 2), which partially interrupts the conjugation, increases the solubility and decreases the conductivity along the chain. When the PAI oligomers are exposed to the doping agent, the UV-visible spectra show two energies, which are assigned to the aromatic part (298 nm) and the delocalization of the π-electrons in the ring (367 nm). In this case, the band gap (Fig. 1(d)) decreases with increasing conjugation length, as is evident from Table 1.

Molecular mass

MALDI-TOF mass spectrometry has become an essential tool for the characterization of synthetic polymers.[39–41] This technique can be used to obtain the absolute molecular mass distributions

Table 2. Average molecular mass for PAI oligomers obtained from MALDI-TOF mass spectrometry

Oligomer	Repeat unit (g mol^{-1})	Observed *m/z*	Molecular mass (g mol^{-1})
PALA	948	2886	2862
PALL	1032	3114	3113
PALPHA	1004	2022/2044	2021
PALV	1100	3381	3358

Table 3. Raman spectral data and thermal behavior[a] of PAI oligomers

	Raman spectroscopy		DSC		TGA	
Oligomer	Onset (°C)	T_g (°C)	Onset (°C)	T_g (°C)	IDT (°C)	T_{10} (°C)
PALA	136	142	144	152	360	394
PALL	106	102	104	118	283	352
PALV	128	135	134	144	298	376
PALPHA	152	156	145	150	398	418

[a] IDT, initial decomposition temperature (5% mass loss); T_{10}, temperature of 10% mass loss; T_g, glass transition temperature.

for polymers systems. The molecular masses obtained for the PAI oligomers prepared are given in Table 2.

For some samples, it is possible to observe *m/z* signals which are assigned to protonated species; for other samples, their *m/z* signals are assigned to protonated species and to sodium salts. From the observed *m/z* signals the resulting PAI oligomers show molecular masses ranging from 2021 to 3358 g mol^{-1}. These compounds are constituted of three repeat units for PALA, PALL and PALV, and two repeat units for PALPHA. In both cases the low molecular masses observed indicate the formation of oligomers. Additionally, PALPHA has a low molecular mass due to structural steric hindrances. In this case, the internal rotation of the phenyl group from the amino acid moiety could hinder the polymerization process.

Thermal analysis and study of glass transition using Raman spectroscopy

From the respective thermograms, temperatures of 5 and 10% mass loss for the PAI oligomers were calculated. The TGA measurements reveal that all samples exhibit good thermal stability. They begin to decompose in the range 283–398 °C in air atmosphere, as indicated by the temperature of 5% mass loss (IDT). The temperature of 10% mass loss is in the range 352–418 °C. In accordance with Table 3, it is clear that PALPHA has higher thermal stability and rigidity than the other samples due to the L-Phe moiety incorporated as chiral center into the polymer chains. Additionally, PALV and PALL exhibit a further degradation due to the reduced packing efficiency produced by the presence of flexible units of aliphatic chains.

To understand the glass transition from a different analytical viewpoint, Raman spectroscopy was used to study the evolution of specific vibrations as a function of temperature (C═C and C═O stretching). The spectra are shown in Fig. 2. The area of the Raman peaks represents the amount of molecular vibrations (phonons) with specific energies. Therefore, this represents a key parameter

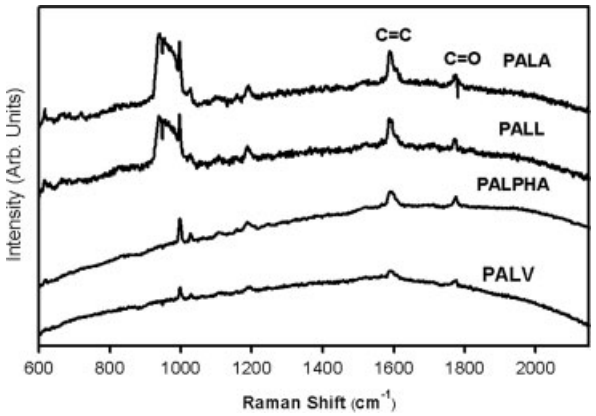

Figure 2. Raman spectra of the PAI oligomers at room temperature showing the peaks corresponding to C═C (1590 cm^{-1}) and C═O (1770 cm^{-1}) stretching.

for the study of thermodynamic transitions. In particular, the glass transition is caused by changes in the microscopic dynamics, due to small momentum transfer that corresponds to correlations larger than the short-range order in the system. When a PAI oligomeric film is heated in the glass transition range, motions at the atomic and molecular scale produce changes in the Raman peak area. These changes are associated with the movements of twisting angles, which are sterically hindered due to the presence of phenyl groups. Thus, when the rings are coplanar, the area obtained from Raman analysis suffers an inflection (minimum or maximum) around the glass transition.[22] This last idea is in agreement with previous work,[19] where an explicit dependence of T_g with the thickness of thin films is reported. If the polymer average end-to-end distance is much smaller than the total thickness, then the dependence would be weak, due to the loss of the confinement effect. Our results show that the powder sample size is three orders of magnitude greater than the PAI oligomeric end-to-end distance. Thus we expected to observe two possible anomalies, corresponding to the bulk and surface transitions.

Figure 3 shows DSC thermograms and plots of the area of the Raman peaks obtained by Gaussian fits. Also, Table 3 summarizes the corresponding T_g values. Two inflection points (minimum) are observed for C═C aromatic bending (1590 cm^{-1}) in PALA (Fig. 3(a)), and for C═O imide stretching (*ca* 1772 cm^{-1}) in PALL (Fig. 3(b)) and PALV (Fig. 3(c)). These observations are associated with the glass transition of surface (low temperature) and bulk (high temperature), as has been reported by Liem and co-workers.[19,22] PALPHA shows an interesting behavior for C═O imide stretching (1773 cm^{-1}), and similar to the DSC curve (Fig. 3(d)). In this case, the low-temperature point is determined by the inflection of the peak area *versus* temperature curve, since the sign of the rate (derivative) also switches from negative to positive values.

It is important to note that the T_g values obtained from DSC for PALA, PALL and PALV are between surface and bulk T_g values, determined by Raman spectroscopy. However, the presence of a phenyl group as pendent element in the main chain of PALPHA not only produces higher T_g (DSC) than for the other samples, but also increases the temperature of the surface and bulk glass transitions (Raman). The phenyl group limits chain movement, which produces a high rigidity of the structure. Probably, this behavior explains the inflection observed instead of a minimum as for the other samples.

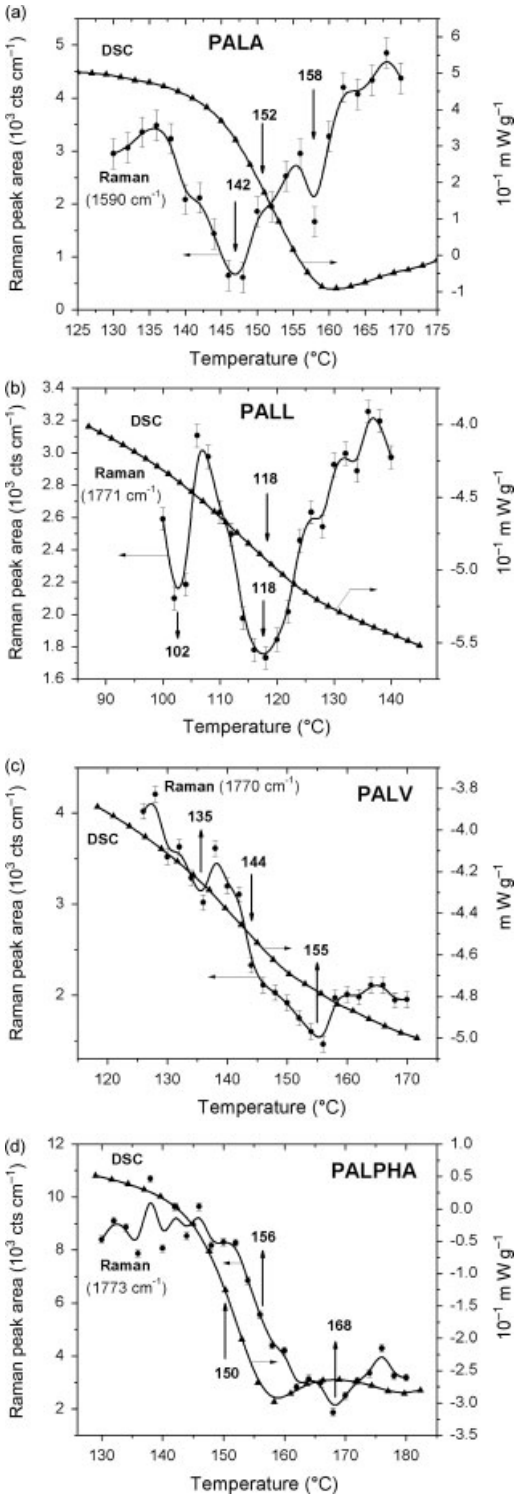

Figure 3. DSC curves and plots of the area of the Raman peaks obtained by Gaussian fits.

Conductivity measurements: conductance–voltage curves

An RT66B electronic tester (Radiant Technologies Inc.) was used to obtain current–voltage curves in order to study the electrical conductance of the PAI oligomers. Silver electrodes were deposited by PVD on the bottom and on half of the top side of oligomeric pellets. In addition, silver paint was used to fabricate

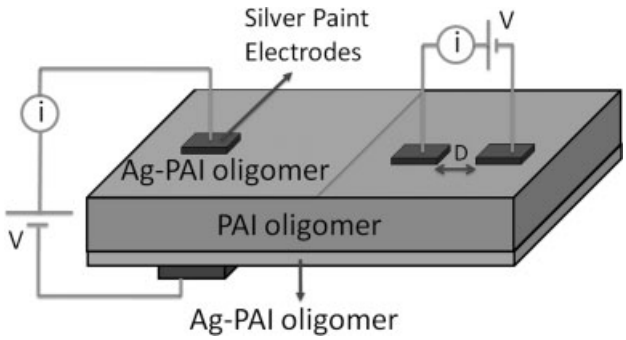

Figure 4. Schematic of the measurement of conductivity.

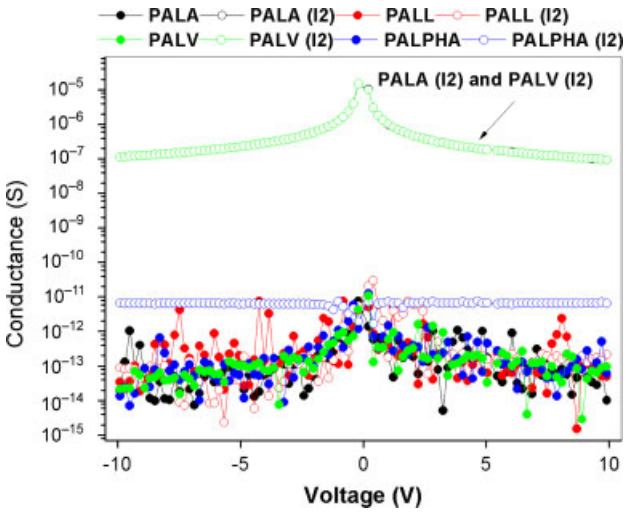

Figure 5. Measurement of conductance using circuit 1 (see Fig. 4).

electrodes smaller than 0.02 cm^2 and separated by distances larger than 0.5 mm. The voltage was varied from 0 to 10 V, and then from 0 to −10 V, in steps of 0.2 V. Thus, the current (*i*) was measured on both surfaces: Ag–PAI oligomer (circuit 1) and PAI oligomer only (circuit 2).The measuring time (soak time) per step was 0.1 s. As shown in Fig. 4, the measurements of conductivity were performed for two different circuits: circuit (1) uses electrodes of Ag–PAI oligomer above and below the pellet; circuit (2) has silver paint electrodes above the PAI oligomer surface.

At room temperature, samples without doping exhibit conductance in the range 10^{-14} to 10^{-13} S, indicating the presence of disordered regions within the material. After doping, the charge carriers are introduced by oxidation of the chains and a delocalization of π-electrons occurs increasing the conductance. This behavior is observed for PALV and PALA (Fig. 5) and might be related to the higher regioregularity in the system, consisting of highly ordered microdomains. Moreover, PALL and PALPHA previously exposed to iodine vapor (PALL(I_2) and PALPHA(I_2), respectively) show a lower value of conductance. In these samples, the main chains have a random orientation due to the flexibility conferred by the $-CH_2-$ units and possible steric hindrance of the phenyl group. Due to these groups, the chains will be heterogeneously oriented in the plane, affecting the morphology and also the conductance of the system.

Lower values of conductance are found after measuring on the surface (Fig. 6) using circuit 2 (see Fig. 4). This could be due to the possible random in-plane orientation produced by disorders

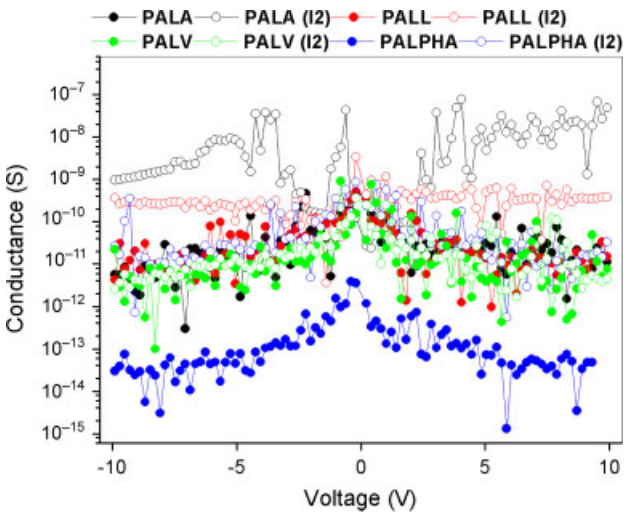

Figure 6. Measurement of conductance using circuit 2 (see Fig. 4).

of the microdomains consisting of stacked wires that are mainly conducting in the longitudinal direction (along the π-bonds) of the main chain. This fact demonstrates that the conductivity may be affected by a certain electrical and optical anisotropy.

It is possible to conclude that, in these systems, the electron mobility measured as conductance is affected by structural anisotropies, which can also affect optical properties, as discussed in a previous section.

CONCLUSIONS

A series of new optically active PAI oligomers were synthesized by direct polycondensation and structurally characterized using elemental analysis and spectroscopic techniques (FTIR, Raman and NMR). These samples were thermally stable and completely soluble, at room temperature, in common organic solvents. These properties were influenced by the presence of the chiral group in the main chain as a pendent group.

Raman spectroscopy was used as an additional tool for studying the glass transition in the PAI oligomeric films. A maximum difference of 12% was observed between the T_g values obtained from DSC and Raman analyses.

Using MALDI-TOF mass spectrometry it was possible to obtain the statistical distribution of the molecular masses of all samples and the numbers of repeat units of which they are comprised.

The conductance variations observed are mainly related to geometrical effects, which include disordered and ordered regions within the system. This would indicate that the alignment of the molecules is a crucial factor for the electrical properties and therefore for the electrical performance. However, when the PAI oligomers are exposed to iodine vapor, charge transfer may increase their mobility and then their optical band gaps can be decreased. This interesting property highlights the possibility of generating alternative active optoelectronics materials.

ACKNOWLEDGEMENTS

The authors are grateful for the financial support provided by MECESUP UCH 0601 and FONDECYT (grants 1100015, 1095151, 1100882).

REFERENCES

1 Kriecheldorf HR and Gurau M, *J Polym Sci A: Polym Chem* **33**:2241–2250 (1995).
2 Liaw DJ and Liaw BY, *J Polym Sci A: Polym Chem* **36**:2301–2307 (1998).
3 Liaw DJ, Liaw BY and Chen YS, *Polymer* **40**:4041–4047 (1990).
4 Liaw DJ, Liaw BY, Sillion B, Mercier R, Thiria R and Sekiguchi H, *Polym Int* **48**:473–478 (1999).
5 Liaw D, Hsu P and Liaw B, *J Polym Sci A: Polym Chem* **39**:63–70 (2001).
6 Babooram K, Francis B, Bissessur R and Narain R, *Compos Sci Technol* **68**:617–624 (2008).
7 Liaw D and Liaw B, *Polymer* **42**:839–845 (2001).
8 Hsiao SH and Yang CP, *J Polym Sci A: Polym Chem* **28**:1149–1159 (1990).
9 Liaw D and Chen W, *Polym Degrad Stab* **91**:1731–1739 (2006).
10 Barikani M and Ataei SM, *J Polym Sci A: Polym Chem* **37**:2245–2250 (1999).
11 Wang Y, Goh S, Chung T and Na P, *J Membr Sci* **326**:222–233 (2009).
12 Ventura G, Gottardi E, Peroni I, Peruzzi A and Ponti G, *Nucl Phys B Proc Suppl* **78**:571–572 (1999).
13 Li F, Ge JJ, Honigfort PS, Fang S, Chen JC, Harris FW, *et al*, *Polymer* **40**:4987–5002 (1999).
14 Hamciuc C, Hamciuc E and Bruma M, *Mater Plast* **35**:75–81 (1998).
15 Bøggild P, Grey F, Hassenkam T, Greve DR and Bjøenholm T, *Adv Mater* **12**:947–950 (2000).
16 Kowalik J, Tolbert LM, Narayan S and Abhiraman AS, *Macromolecules* **34**:5471–5479 (2001).
17 Wu P-T, Bull T, Kim FS, Luscombe ChK and Jenekhe SA, *Macromolecules* **42**:671–681 (2009).
18 Vignaud G, Bardeau JF, Gibaud A and Grohens Y, *Langmuir* **21**:8601–8604 (2005).
19 Liem H, Cabanillas-Gonzalez J, Etchegoin P and Bradley DDC, *J Phys: Condens Matter* **16**:721–728 (2004).
20 Murai M, Nakayama H and Ishii K, *J Therm Anal Calorim* **69**:953–959 (2002).
21 Stavrou E, Tsiantos C, Tsopouridou RD, Kripotou S, Kontos AG, Raptis C, *et al*, *J Phys: Condens Matter* **22**:195103 (2010).
22 Liem H, *J Phys: Condens Matter* **19**:416106 (2007).
23 Schulz B, Hamciuc E, Köpnick T, Kaminorz Y and Bruma M, *Macromol Symp* **199**:391–400 (2003).
24 Bruma M, Hamciuc E, Sava I and Belomoina N, *Russ Chem Bull* **53**:1813–1823 (2004).
25 Hamciuc E, Hamciuc C, Sava I and Bruma M, *Eur Polym J* **37**:287–293 (2001).
26 Okamoto Y and Yashima E, *Prog Polym Sci* **15**:263–298 (1990).
27 Yashima E, Maeda K and Okamoto Y, *Nature* **399**:449–451 (1999).
28 Pratt JR and Thames SF, *J Org Chem* **38**:4271–4274 (1973).
29 Tagle LH, Terraza CA, Leiva A and Devilat F, *J Appl Polym Sci* **110**:2424–2431 (2008).
30 Tagle LH, Terraza CA, Leiva A, Yazigi N and López L, *J Appl Polym Sci* **117**:1526–1534 (2010).
31 Tagle LH, Diaz FR, Radic D, Opazo A and Espinoza JM, *J Inorg Organomet Polym* **10**:73–79 (2000).
32 Hsiao S-H, Yang C-P and Chu K-Y, *J Polym Sci A: Polym Chem* **35**:1469–1478 (1997).
33 Tundidor-Camba A, Terraza CA, Tagle LH and Coll D, *J Appl Polym Sci* **120**:2381–2389 (2011).
34 Tauc J, Grigorovici R and Vancu A, *Phys Stat Sol B* **15**:627–637 (1966).
35 Gupta S, Choudhary D and Sarma A, *J Polym Sci B: Polym Phys* **38**:1589–1594 (2000).
36 Zaki MF, *Braz J Phys* **38**:558–562 (2008).
37 Fox M, *Optical Properties of Solids*. Oxford University Press, New York (2001).
38 Shujiang Y, Pavel O and Miklos K, *Synth Met* **141**:171–177 (2004).
39 Crecelius AC, Baumgaertel A and Schubert US, *J Mass Spectrom* **44**:1277–1286 (2009).
40 Weidner SM and Trimpin S, *Anal Chem* **80**:4349–4361 (2008).
41 Lloyd PM, Suddaby KG, Varney JE, Scrivener E, Derrick PJ and Haddleton DM, *Eur J Mass Spectrom* **1**:293–300 (1995).